J. Earth Syst. Sci. (2020)129 39
https://doi.org/10.1007/s12040-019-1301-8

Composition of the peninsular India rivers average clay (PIRAC): A reference sediment composition for the upper crust from peninsular India

Shaik Sai Babu[1], Ravipati Venkata Ramana[1], Venigalla Purnachandra Rao[1,*], Mekala Ram Mohan[2], Aradhi Keshav Krishna[2], Saripoot Sawant[2] and Nannapaneni Satyasree[1]

[1] *Vignan's Foundation for Science, Technology and Research (VFSTR), Deemed-to-be Vignan's University, Vadlamudi, Guntur District, AP 522 213, India.*
[2] *CSIR–National Geophysical Research Institute, Uppal Road, Hyderabad 500 007, India.*
**Corresponding author. e-mail: vprao55@gmail.com*

MS received 8 July 2019; revised 6 September 2019; accepted 10 September 2019

We present a new dataset on the average composition of the clay fraction of sediments in 13 rivers draining the entire peninsular India, referred to here as Peninsular India Rivers Average Clay (PIRAC). PIRAC showed relatively low Si and high Fe, Mn and Mg compared to the other reference sediments. The total trace elements ($\sum$TE) content of PIRAC was lower than that of Post-Archean average Australian Shale (PAAS), but close to that of Average Suspended Sediment of World Rivers (ASSWR). The total rare earth elements ($\sum$REE) content of PIRAC was slightly lower than that of PAAS but close to that of World River Average Clay (WRAC). The $\sum$TE and $\sum$REE were much higher for PIRAC than in other reference sediments. Anomalously high Cu, Zn and Pb in PIRAC suggest that these trace elements do not reliably indicate the crustal composition. PAAS-normalised REE of PIRAC showed LREE-depleted, MREE- and HREE-enriched REE patterns with positive Ce and Eu anomalies, suggesting that PIRAC is more mafic than that of PAAS and the clays weathered from volcanic rocks and felsic component of the metamorphic rocks dominated the crustal composition of peninsular India. The REE pattern of PIRAC resembles to that of European Shale (ES) and Mud of Queensland (MUQ) but different from PAAS, WRAC, upper continental crust (UCC) and East China Post-Archean Shale (ECPAS), which exhibit LREE-enriched and HREE-depleted REE patterns. It implies that the REE composition of the upper crust is not uniform and it should be thoroughly investigated to determine the composition of PIRAC with more analyses on sediments for better understanding of the evolution of the crust.

Keywords. Upper crust; peninsular India; reference sediment; trace elements; REE.

1. Introduction

The upper continental crust (UCC) consists of sedimentary cover (sediments/sedimentary rocks) and the underlying metamorphic or volcanic basement rocks. The geochemistry of the near surface sediments/sedimentary rocks provides information on the composition of the upper crust and, determining sediment composition has been an important pursuit of geologists for understanding of the chemical evolution of the Earth's crust (McLennan 2001). Condie (1993) suggested that

Published online: 30 December 2019

the average major element composition of the upper crust is similar to the average granodiorite, while much of the lower crust may be basaltic in composition and the average composition of the bulk continental crust may be misleading in reconstructing the upper crustal history. The sediments preserve record of their sources and allow us to examine the relationship between the composition of upper crustal sources and nature and distribution of sediments.

The composition of sediments usually depends on the (a) lithological composition of the crustal rocks, (b) type and intensity of weathering, (c) effect of sedimentary sorting and (d) diagenesis (McLennan *et al.* 2001). The major and trace elements are widely used to evaluate the composition of sediments (Absar *et al.* 2009). The sediments usually represent not only a single source rock but admixture of different lithologies, and absolute abundances of elements reflect the proportions of lithologies in the catchment. Major element composition of the sediments changes greatly with the sediment constituents, grain size and weathering. Trace elements chemistry is controlled by source rocks and intensity of weathering (Zhao and Zheng 2015). Some elements with high solubilities in water are fractionated rapidly during sedimentary processing and, elements with low solubilities are incorporated in secondary minerals such as clays or oxy-hydroxides (Taylor and McLennan 1985). The trace element geochemistry of sediments from highly weathered catchments differs from that of the unweathered bedrocks not only in absolute concentration but also in relative abundance (Taylor and McLennan 1985). Viers *et al.* (2009) reported that the trace elements in suspended loads of rivers draining temperate regions are different from that of tropical rivers. Moreover, trace element concentrations are to be affected by processes such as pollution, loss to hydrosphere or mineralogical sorting (Taylor and McLennan 1985). Thus, the major and trace elements in the sediments are to be affected by sedimentary processes and may not reliably indicate the crustal composition. On the other hand, Rare Earth Elements (REE) have been widely used to identify source sediments. It has been assumed that REE are not easily fractionated but transferred near quantitatively in terrigenous sediments during erosion and sedimentation. Thus, the REE patterns of sediments may provide an index of average provenance composition (Absar and Sreenivas 2015; Rashid *et al.* 2018). The sedimentary REE patterns are generally uniform in comparison to potential igneous/metamorphic source rocks and are interpreted as resulting from efficient mixing of various provenance components from the upper crust (Cullers *et al.* 1979; Bhatia *et al.* 1985; McLennan *et al.* 2001). Subsequently, it was realized that several factors, including source rocks, grain size, mineralogy and heavy minerals content influence both REE abundance and REE patterns. For example, it was found that bulk REE reside largely in silt and clay fraction of sediments and, silts tend to have lower abundances compared to that of clay (Cullers *et al.* 1979; Bayon *et al.* 2015). The sediments rich in heavy minerals such as zircon exhibit high total-REE content and HREE-enriched patterns (Jung *et al.* 2012; Marchandise *et al.* 2014). More HREE are removed to the solution during intense chemical weathering. With increasing number of chemical analyses on crustal sediments from different regions, more variability has been observed on REE distribution.

The average REE composition of the terrigenous sediments is widely accepted to reflect upper continental crust. In this respect, the average chemical composition of the upper continental crust (UCC – Taylor and McLennan 1985; McLennan 2001; Rudnick and Gao 2003) and Post-Archean average Australian Shale (PAAS – Nance and Taylor 1976; Pourmand *et al.* 2012) have been published and are being used as reference sediments that represent the composition of upper crust and for comparison in a number of geochemical studies. The REE pattern of UCC is parallel to that of PAAS, but lower in absolute abundances due to the presence of sediments with lower REE abundances, such as sandstones, carbonates and evaporites (McLennan 2001). Studies on REE distribution in shales and other sedimentary and meta-sedimentary rocks have been extended to include samples from most of the continents, from a variety of geological environments and materials as old as the earliest Archean. These studies have confirmed that the Post-Archean sediment composites as a group have rather uniform (Gromet *et al.* 1984) REE characteristics, although sediments with sources restricted to certain limited environments can deviate considerably from these values. The reference sediments include North American Shale Composite (NASC – Gromet *et al.* 1984), European Shale (ES – Haskin and Haskin 1966), Mud of Queensland (MUQ – Kamber *et al.* 2005), East China Post-Archean Shale (ECPAS – Gao *et al.* 1998), composition of the Average Suspended

Sediments of World Rivers (ASSWR – Viers *et al.* 2009) and REE compositions of World River Average Clay (WRAC – Bayon *et al.* 2015). From the results of above investigations, one can understand that the REE patterns of shales vary and depend on the mineral composition and grain size of the sediments. REE patterns of the fine-grained sediments are more consistent and reliable because REE reside largely in clay and silt fractions of sediments (Bayon *et al.* 2015). Further, it has been reported that the REE of silt fraction shows uniform composition, while the clay fraction shows more variability in REE composition depending on mineral composition (Bayon *et al.* 2015). Several reference sediments, although available from different sub-continents and World's major rivers, there is a lack of data on the average composition of crust from the Indian subcontinent or peninsular India. The aim of this paper is to present dataset of geochemical compositions of the clay fraction of sediments in 13 medium and major rivers (figure 1; table 1) and report the average composition of the crust for the Indian subcontinent, referred to here as Peninsular India Rivers Average Clay (PIRAC). The composition of PIRAC was also compared with other reference sediments. We would like to mention here that it is the beginning to prepare database for the crustal composition of the peninsular India and will update the database with increased number of analyses.

1.1 *Geology of the peninsular India*

The geology of peninsular India and rivers that drain the entire Indian subcontinent are shown in figure 1. The terms 'major' and 'medium' rivers are adopted from Rao (1975). Major rivers are those with drainage basin area >20,000 km^2, while the medium rivers are those with drainage basin area between 20,000 and 2,000 km^2. The major or medium rivers along the east coast of India, originate in the Western Ghats (mountain ranges) (figure 1) or in the west and transport huge sediment (both suspended and bed) load to the east coast of India, primarily because of the morphotectonic slope from the west to the east of India (Krishnan 1968). The dominant geological formations in the drainage basins of rivers in the entire peninsular India can be broadly categorised into three major terrains: Archean–Precambrian Terrain (APT), Deccan Trap Volcanic Terrain (DVT) and Mixed-lithology (both igneous and metamorphic rocks) Terrain (MLT). Among the six rivers draining APT, the Cauvery, Ponnaiyar, Palar and Pennar rivers drain Dharwar Craton and Southern Granulite Terrain (SGT) in the upper and middle reaches and, Cenozoic formations and Cretaceous sandstones and limestones in the lower reaches (Balakrishnan and Rajamani 1987; Srinivasan *et al.* 1989; Sharma and Rajamani 2000; Singh and Rajamani 2001; Naqvi 2005; Bhattacharya *et al.* 2012). The Dharwar Craton consists of greenstone schists, gneisses, charnokites and younger granites. The Southern Granulite Terrain consists of Archaean to Neoproterozic high grade metamorphic rocks (charnokites, granite gneisses and migmatites). The Nagavali and Vamsadhara rivers originate in the Eastern Ghats and drain Precambrian khondalites consisting of quartz, sillimanite and garnet-rich schists, gneisses and granulites (Dash *et al.* 1987). Mn ores and Mn–Fe oxide deposits are associated with the khondalites (Moriyama *et al.* 2008). The Krishna, Vasishta Godavari and Gautami Godavari Rivers drain Deccan Trap Volcanic Terrain (DVT) in the upper reaches and Precambrian gneisses and schists and deltaic sediments in the lower reaches (Krishnan 1968). Similarly, the Mahanadi, Brahmani, Baitarani and Subarnarekha Rivers drain Mixed-Lithology Terrain (MLT) consisting of metamorphic and igneous rocks and soils. The geological formations in the MLT are Paleo-archaean high grade metamorphic rocks and Archaean low-grade metamorphic iron ore group of the Singhbhum Craton. The continental crust in the Singhbhum region is marked by emplacement of older metamorphic Tonalite gneisses. The chromite deposits are part of the iron ore group. Dacitic lava formed in a volcanic arc setting is well preserved in the southern iron ore group of Singhbhum Craton. Thus, these rivers drain through the ore deposits of Mn, Fe–Mn, Cr oxides and Cu, Zn and Pb sulphides in the upper reaches and gneissic rock types and red, yellow and black soils, lateritic soils and deltaic soils in the lower reaches (Ray *et al.* 1984; Konhauser *et al.* 1997). Tropical climate prevails over the peninsular India and as a consequence chemical weathering is predominant (Nesbitt *et al.* 1990). In other words, the rivers erode and drain different geological formations under tropical conditions and the weathered products get mixed-up, recycled during transportation and ultimately deposited at the river mouth and on the continental margins. The fine fraction of sediments deposited at the river mouth thus represent the composition of the upper crust.

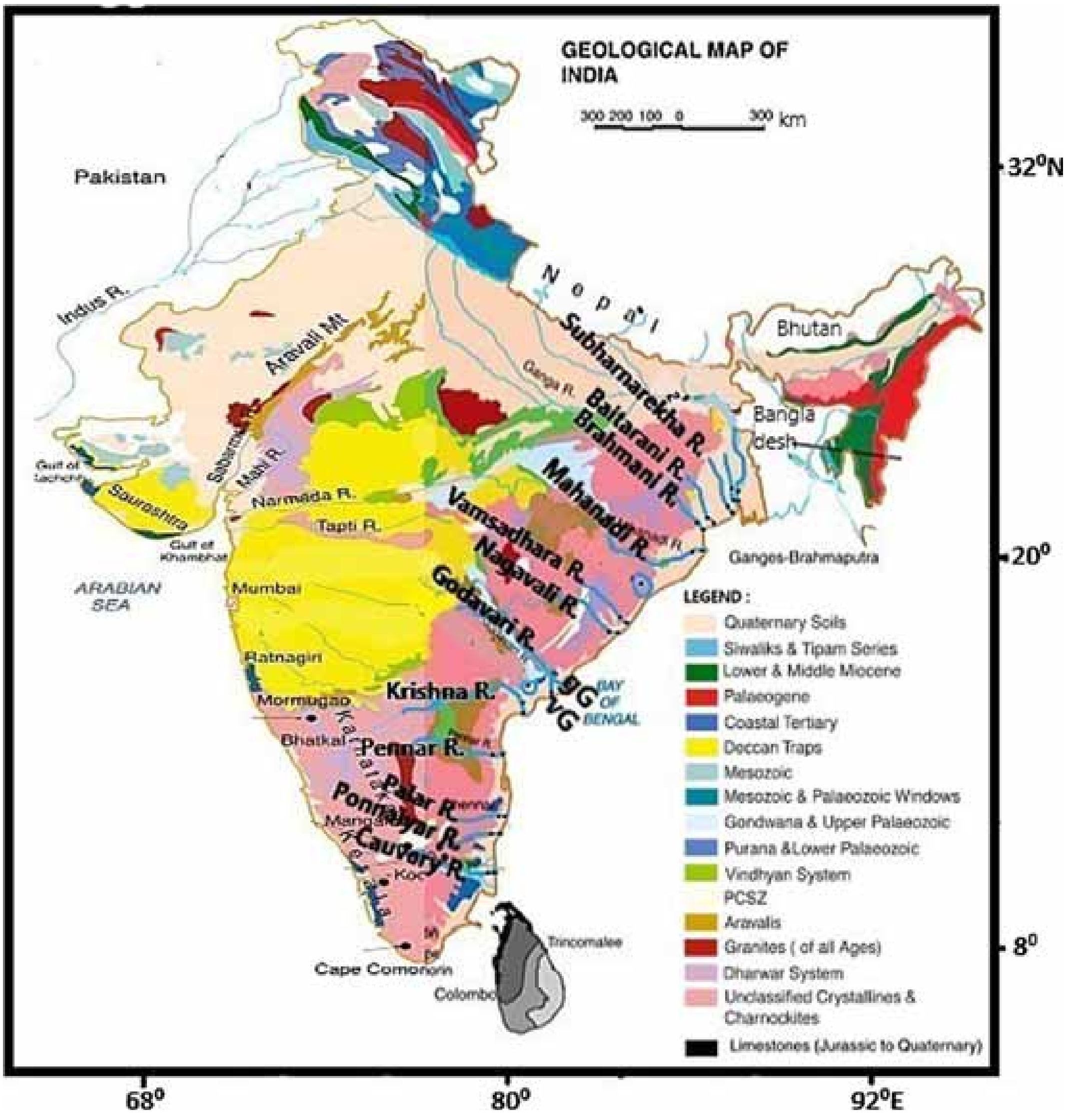

Figure 1. Generalised geological map of India. Rivers draining various geological formations are also shown (GSI 1998). *Medium rivers with catchment area between 2000 and 20,000 km^2. **Major rivers with catchment area >20,000 km^2 (this terminology is based on Rao 1975).

2. Materials and methods

Sediments from lower reaches of the rivers and ∼5 km landward of their estuaries were collected in 13 medium and major rivers along the east coast of India, using Peterson grab and with the help of a mechanized boat. The sediments were dried in an oven at <60°C. Since fine-grained sediments better represent the crustal composition, the clay fraction (<4 μm) of sediments was separated based on settling velocity principle, dried and powdered. These powders were used for chemical analyses. One gram of dried sample powder was used to prepare pellets and major elements were determined, using X-ray fluorescence spectrometer (XRF), using the instrument 'WD-XRF' Model Axios mAX, PANalytical at the CSIR–National Geophysical Research Institute (CSIR–NGRI), Hyderabad. For the trace elements, 50 mg of the homogenized powdered sediment sample was transferred into Teflon beaker and 10 ml of acid mixture (7:3 of HF and HNO_3) was added to each beaker, kept overnight on a hot plate at 150°C for 48 hrs. Two drops of $HClO_4$ were added to the beaker and evaporated at 150°C for ∼1 hr to near dryness. This procedure was repeated till the sample in the beaker was completely digested. The final residue was dissolved in 10 ml of 1:1 of water and HNO_3 mixture and subsequently 5 ml of 1 ppm Rh^{103} solution was added to the beaker as an internal standard and final volume of the sample solution was made up to 250 ml. The instrument

Table 1. *Major (%) and trace element (μg/g) contents in <4 μm fraction of sediments in rivers along the east coast of India.*

	Archean and Pre-cambrian Terrain							Deccan Trap Volcanic Terrain				Mixed Lithology Terrain					Reference sediments								
Element	Cauvery**	Ponnaiyar*	Palar*	Pennar**	Nagavali*	Vamsadhara*	Average	Krishna**	Vasishta Godavari**	Gautami Godavari**	Average	Mahanadi**	Brahmani**	Baitarani*	Subharnarekha*	Average	PIRAC	WRAC	ASSWR	PAAS	ECPAS	MUQ	NASC	ES	UCC
SiO_2	52.35	52.49	52.91	55.96	53.46	53.35	53.42	51.86	54.46	51.70	52.67	58.21	53.19	56.93	56.31	56.16	54.09	52.09	51.90	62.80	67.97	67.53	64.80	–	66.20
Al_2O_3	18.62	19.71	17.92	17.68	22.03	22.95	19.81	15.83	17.18	22.16	18.39	20.10	22.18	20.60	20.84	20.93	19.83	21.84	16.50	18.9	14.17	17.31	16.90	–	15.30
Fe_2O_3	13.07	11.75	12.73	12.27	11.46	12.15	12.23	14.55	14.50	14.12	14.39	10.68	12.24	11.70	11.24	11.46	12.49	8.80	8.30	7.22	5.33	7.77	12.67	–	5.57
MnO	0.16	0.11	0.58	0.30	0.22	0.12	0.24	0.19	0.14	0.15	0.16	0.07	0.17	0.16	0.18	0.14	0.19	0.05	0.20	0.11	2.62	0.14	0.06	–	0.09
CaO	1.83	1.91	0.93	1.55	0.39	0.36	1.16	1.46	1.01	1.08	1.18	0.36	0.40	0.62	0.49	0.46	0.95	0.53	3.60	1.30	3.44	1.10	3.63	–	3.57
MgO	2.77	4.39	3.99	4.24	2.33	2.29	3.33	5.27	4.39	2.69	4.11	2.32	2.59	3.00	3.37	2.82	3.35	2.59	2.10	2.20	0.10	1.57	2.86	–	2.47
K_2O	1.72	1.59	1.65	2.43	2.16	2.51	2.01	1.91	2.24	1.94	2.03	2.70	2.47	2.74	3.24	2.78	2.25	2.91	2.00	3.70	2.68	1.54	3.97	–	2.78
Na_2O	0.64	1.80	1.52	1.27	0.82	1.53	1.26	3.55	3.05	3.23	3.28	0.61	1.55	2.10	1.56	1.45	1.78	0.65	1.00	1.20	2.86	0.80	1.14	–	3.25
TiO_2	1.72	0.78	0.76	0.89	0.85	0.72	0.95	1.28	1.58	1.12	1.32	1.09	1.07	0.96	0.93	1.01	1.05	0.87	0.70	1.00	0.67	1.36	0.70	–	0.65
P_2O_5	0.55	0.18	0.25	0.22	0.20	0.21	0.26	0.12	0.13	0.21	0.15	0.17	0.17	0.16	0.17	0.16	0.21	0.34	0.50	0.16	0.16	0.18	0.13	–	0.15
LOI	7.13	5.11	6.60	3.04	5.82	3.65	5.22	3.86	1.33	1.43	2.20	3.53	3.81	1.04	1.51	2.47	3.68	–	–	–	–	–	–	–	–
CIA	81.63	79.80	81.38	77.10	86.75	85.91	81.59	69.58	73.16	77.94	73.56	84.56	83.38	79.04	79.75	81.68	79.76	84.22	71.42	75.29	61.20	83.42	65.91	–	61.44
CIW	88.28	84.15	87.97	86.24	94.79	92.39	88.97	75.95	80.88	83.65	80.16	95.39	91.81	88.33	91.04	91.66	87.76	94.87	78.19	88.31	69.22	90.10	77.98	–	69.16
Sc	13.32	13.11	12.85	17.64	23.79	21.04	16.96	23.89	25.92	24.28	24.70	20.99	19.17	20.45	14.89	18.87	19.33	–	18.20	15.89	15.00	16.49	14.90	–	14.00
V	92.53	71.72	89.36	100.06	118.76	104.90	96.37	186.74	201.09	156.52	181.45	133.50	141.72	122.33	94.87	123.11	124.23	–	129.00	150.00	98.00	120.00	–	–	97.00
Cr	168.91	119.18	110.40	113.04	105.39	100.03	119.49	117.10	128.27	142.33	128.57	117.76	142.52	137.49	101.38	124.79	123.22	–	130.00	110.00	80.00	84.50	125.00	–	92.30
Co	25.28	19.28	25.29	24.80	38.89	22.35	25.98	31.04	31.14	33.86	32.01	20.37	40.87	22.79	19.58	25.90	27.35	–	22.50	23.00	17.00	22.39	–	–	17.30
Ni	84.93	66.84	61.86	75.33	66.16	62.92	69.67	75.38	72.82	77.17	75.13	58.43	70.21	65.42	58.12	63.05	68.89	–	74.50	55.00	38.00	31.57	58.00	–	47.30
Cu	214.91	1068.13	543.39	151.89	137.37	458.68	429.06	151.29	206.77	228.60	195.55	73.18	70.28	57.27	104.41	76.29	266.63	–	75.90	50.00	32.00	32.36	–	–	27.70
Zn	1103.14	1519.36	751.85	386.43	274.02	624.68	776.61	467.08	366.50	391.23	408.27	137.38	113.83	199.89	186.01	159.27	501.66	–	208.00	85.00	70.00	73.47	–	–	67.00
Ga	11.87	12.87	12.76	17.56	17.97	18.30	15.22	16.52	19.24	20.69	18.82	21.40	21.89	20.68	15.79	19.94	17.50	–	18.10	20.00	18.00	19.12	–	–	17.50
Rb	47.68	52.44	56.47	112.74	77.66	124.64	78.61	68.56	98.48	94.06	87.03	139.21	99.79	135.60	112.49	121.77	93.83	–	78.50	160.00	82.00	79.51	125.00	–	82.00
Sr	116.90	172.29	98.73	121.99	75.08	68.40	108.56	98.94	75.41	124.79	99.71	68.62	47.38	78.51	62.62	64.28	82.90	110.00	187.00	200.00	266.00	142.00	142.00	–	320.00
Y	27.45	19.53	18.48	26.52	60.49	50.09	33.76	27.39	35.72	44.29	35.80	42.96	27.54	35.13	26.74	33.09	34.02	29.84	21.90	27.31	17.40	31.85	27.00	31.80	21.00
Zr	47.72	49.06	45.15	102.34	56.35	63.01	60.60	119.03	129.75	110.91	119.90	103.96	84.37	95.81	65.94	90.02	83.34	148.00	160.00	210.00	188.00	199.00	200.00	–	193.00
Nb	5.68	4.89	4.75	9.01	6.49	6.66	6.25	7.20	9.69	11.24	9.38	12.53	12.00	10.93	7.96	10.86	8.39	–	13.50	19.00	12.00	15.33	–	–	11.80
Cs	1.51	1.62	1.86	6.41	3.43	4.84	3.28	3.71	4.90	4.76	4.46	8.68	8.90	9.58	8.10	8.81	5.25	–	6.25	15.00	3.55	5.38	5.00	–	4.10
Ba	358.57	235.45	189.59	277.55	439.51	319.12	303.30	130.67	200.55	325.63	218.95	332.97	549.51	272.67	257.20	353.09	299.15	380.00	522.00	650.00	678.00	396.00	636.00	–	624.00
La	34.76	35.09	29.71	41.15	45.41	34.12	36.70	23.34	38.18	63.18	41.57	57.54	37.22	48.71	34.96	44.61	40.26	44.61	37.40	44.56	34.80	32.51	32.00	41.10	31.40
Ce	75.56	73.61	65.09	84.84	105.38	73.38	81.31	54.82	81.14	126.78	87.58	118.24	160.24	100.87	73.69	113.26	92.59	89.20	73.60	88.25	66.40	71.09	70.00	81.30	63.40
Pr	7.00	6.91	6.13	8.34	9.42	6.86	7.44	5.30	8.02	11.92	8.42	11.26	6.84	9.63	7.08	8.71	8.05	9.69	7.95	10.15	–	8.46	7.90	10.40	7.10
Nd	29.31	28.10	25.02	33.47	39.52	28.29	30.62	23.26	34.10	48.01	35.12	45.28	25.99	38.65	28.71	34.66	32.90	35.60	32.20	37.32	30.40	32.91	31.00	40.10	27.00
Sm	5.86	5.16	4.76	6.38	8.58	6.43	6.19	5.19	7.35	9.44	7.33	8.95	4.82	7.79	5.83	6.85	6.66	6.70	6.12	6.88	5.00	6.88	5.70	7.30	4.70
Eu	1.44	1.26	1.17	1.39	2.04	1.47	1.48	1.45	1.84	2.26	1.85	1.92	1.10	1.71	1.27	1.50	1.56	1.38	1.29	1.21	1.21	1.57	1.24	1.52	1.02
Gd	5.08	4.02	3.84	5.38	8.95	6.96	5.71	4.96	6.52	8.38	6.62	7.81	4.37	6.84	5.18	6.05	6.02	5.17	5.25	6.04	–	6.36	5.21	6.03	4.01
Tb	0.81	0.62	0.59	0.87	1.65	1.37	0.98	0.86	1.13	1.39	1.12	1.33	0.73	1.13	0.86	1.01	1.02	0.83	0.82	0.89	0.82	0.99	0.85	1.05	0.65
Dy	4.60	3.33	3.19	4.78	9.90	8.36	5.69	4.83	6.35	7.73	6.31	7.40	4.46	6.37	4.71	5.73	5.85	4.87	4.25	5.32	–	5.89	–	–	3.91
Ho	1.00	0.71	0.67	1.02	2.20	1.84	1.24	1.03	1.35	1.64	1.34	1.61	1.02	1.36	1.01	1.25	1.27	0.98	0.88	1.05	–	1.22	1.04	1.20	0.83
Er	2.76	1.85	1.82	2.80	6.28	5.20	3.46	2.82	3.67	4.42	3.63	4.47	2.99	3.72	2.75	3.48	3.51	2.78	2.23	3.07	–	3.37	3.40	3.55	2.30
Tm	0.36	0.25	0.23	0.38	0.82	0.67	0.45	0.36	0.47	0.56	0.46	0.57	0.41	0.48	0.35	0.45	0.45	–	0.38	0.45	–	0.51	0.50	0.56	0.30
Yb	2.41	1.66	1.55	2.40	5.42	4.41	2.98	2.38	3.10	3.58	3.02	3.70	2.85	3.11	2.28	2.98	2.99	2.72	2.11	3.01	2.26	3.25	3.11	3.29	2.04
Lu	0.38	0.26	0.23	0.37	0.84	0.68	0.46	0.36	0.47	0.55	0.46	0.53	0.45	0.47	0.34	0.45	0.46	0.40	0.35	0.43	0.35	0.49	0.48	–	0.30
Hf	1.58	1.59	1.37	2.97	1.63	1.80	1.82	3.31	3.66	3.13	3.38	2.82	2.61	2.59	1.79	2.45	2.37	3.81	4.04	5.00	5.12	5.32	6.30	–	5.26
Ta	0.51	0.48	0.45	0.94	0.63	0.63	0.61	0.74	0.90	1.09	0.91	1.13	1.13	1.06	0.75	1.02	0.80	–	1.27	1.50	0.74	1.12	1.10	–	0.88
Pb	163.19	126.08	69.98	39.95	38.33	41.81	79.89	17.38	23.54	47.34	29.42	34.27	32.91	36.71	40.76	36.16	54.79	–	61.10	20.00	18.00	20.44	–	–	17.00
Th	6.25	7.03	7.07	16.04	10.16	9.61	9.36	7.70	12.51	18.34	12.85	19.76	12.77	18.58	13.62	16.13	12.25	15.10	12.10	14.60	8.95	11.13	2.30	–	10.10
U	1.33	1.40	1.73	2.75	1.43	1.73	1.73	1.74	1.85	2.90	2.16	3.56	2.96	2.56	1.97	2.76	2.15	–	3.30	3.10	1.55	2.83	2.66	–	2.65
ΣREE	171.35	162.93	144.02	203.55	246.43	180.04	184.72	130.98	193.71	289.85	204.84	270.85	255.50	230.85	169.03	231.00	204.23	205.13	175.00	208.66	141.33	175.50	158.02	197.98	148.96
ΣTE	2465.86	3542.98	2082.94	1579.47	1494.1	2055.08	2203.4	1526.03	1611.02	1818.88	1652.64	1310.56	1484.84	1310.77	1168.24	1318.61	1724.88	–	1725.26	1807.20	1631.91	1257.96	158.02	–	1650.87
(ΣLREE)n	3.11	3.06	2.67	3.71	4.2	3.03	3.28	2.29	3.48	5.31	3.69	4.95	4.02	4.22	3.08	4.06	3.47	3.92	3.32	–	2.34	3.23	3.41	3.94	2.84
(ΣMREE)n	5.61	4.46	4.20	5.82	10.22	8.16	6.41	5.65	7.42	9.19	7.41	8.60	4.96	7.44	5.56	6.64	6.54	5.77	5.39	–	2.65	6.72	4.94	5.62	4.43
(ΣHREE)n	3.38	2.34	2.18	3.36	7.58	6.22	4.17	3.34	4.35	5.13	4.27	5.22	3.86	4.39	3.22	4.17	4.04	2.73	3.21	–	1.54	4.42	4.04	4.81	2.77
ΣLREE/ΣHREE	24.81	35.05	32.71	29.98	14.95	13.01	25.08	18.03	20.94	27.43	22.13	25.01	34.37	25.39	25.23	27.5	23.15	30.32	29.64	25.84	–	19.02	18.34	21.66	26.09
(La/Yb)n	0.97	1.42	1.28	1.15	0.56	0.52	0.98	0.66	0.83	1.19	0.89	1.05	0.88	1.05	1.03	1.00	0.90	1.11	1.20	–	1.04	0.67	0.75	0.84	1.10
(Lu/La)n	1.12	0.76	0.81	0.92	1.88	2.05	1.23	1.38	1.25	0.89	1.24	0.98	1.23	0.99	1.00	1.05	1.16	0.92	1.08	–	1.01	1.53	1.29	1.43	0.97
*Ce/Ce	1.08	1.07	1.10	1.14	1.15	1.09	1.10	1.12	1.05	1.04	1.07	1.06	2.31	1.06	1.06	1.37	1.73	1.02	0.98	–	0.94	1.03	0.91	0.93	1.00
*Eu/Eu	1.40	1.49	1.47	1.27	1.24	1.17	1.34	1.52	1.43	1.35	1.43	1.22	1.28	1.25	1.23	1.24	1.54	1.22	1.21	–	–	1.27	0.89	1.23	1.25

PIRAC: Peninsular Indian River Average Clay (this study), WRAC: World River Average Clay (Bayon *et al.* 2015), ASSWR: Average Suspended Sediment in World Rivers (Vier's *et al.* 2009), PAAS: Post Archean average Australian Shale (Talyor and McLennan 1985; Pourmand *et al.* 2012), ECPAS: Eastern China Post-Archean Shale (Gao *et al.* 1998), MUQ: Mud of Queensland (Kamber *et al.* 2005), NASC: North American Shale Composite (Haskin and Haskin 1966; Gromet *et al.* 1984), ES: European Shale (Haskin and Haskin 1966), UCC: Upper Continental Crust (Rudnick and Gao 2003). **Major rivers. *Moderate rivers.

Attom®, High Resolution-Inductively Coupled Plasma-Mass Spectrometer (HR-ICP-MS) from Nu Instruments, UK at the CSIR–NGRI was used for analysis of the sample solutions. MAG-1 (Marine Mud), certified reference material (CRM) from the United States Geological Survey, was used as the calibrating standard for the analysis of the sediments and, JSd-1, CRM for stream sediment from the Geological Survey of Japan was used as cross check standard for the data. Rh^{103} used as an internal standard for instrument drift correction. The details of instrument parameters and HR-ICP-MS analysis with accuracy and precision achieved are given in Satyanarayanan *et al.* (2018). Major elements and trace elements in the clay fraction of sediments in the rivers are shown in table 1. The geochemistry of the sediments reflects varied proportions of lithologies and sedimentary processes in the catchment. The average chemical composition of clay fraction of the sediments in rivers is referred to here as PIRAC. It was calculated by averaging the composition of the clay fraction of sediments in 13 rivers that drained the entire peninsular India. The composition of PIRAC serves as a reference for the sediments of the Indian subcontinent or peninsular India.

3. Results and discussion

3.1 *Major elements*

Table 1 shows the distribution of major and trace elements in the clay fraction of sediments in rivers, their average distribution in three major geological terrains (APT, DVT, MLT) of peninsular India, PIRAC and other reference sediments. The mean major elements distribution in three different terrains (APT, DVT and MLT) were nearly similar to one another or exhibit marginal variations, except that the mean Mn and Ca were slightly lower in MLT and Na was slightly higher in DVT compared to the other two terrains (figure 2a). The major

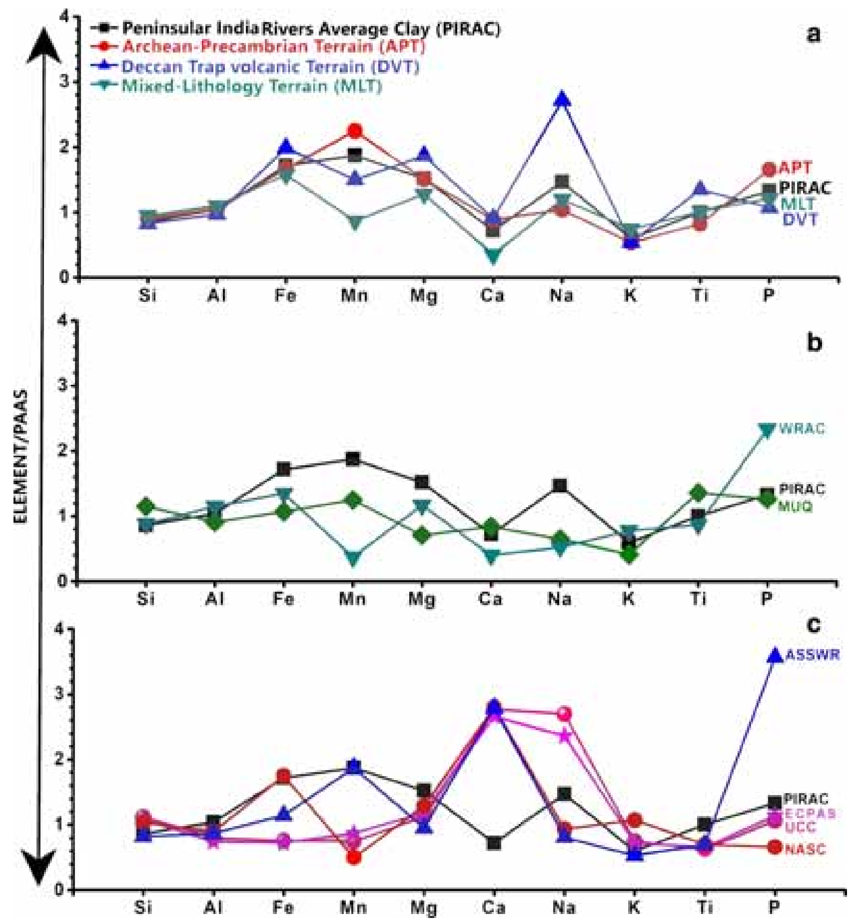

Figure 2. (**a**) Distribution of major elements in three major geological formations and PIRAC. (**b, c**) Distribution of major elements in PIRAC and reference sediments. UCC: Upper Continental Crust, ES: European shale, MUQ: Mud of Queensland, ECPAS: East China Post-Archean Shale, WRAC: World River Average Clay; ASSWR: Average Suspended Sediment of the World Rivers.

elements composition of PIRAC was close to that of APT and DVT. Further, the mean Fe, Mn, Mg and Na contents were higher and Si was lower in PIRAC than in other reference sediments, such as upper continental crust (UCC), Mud of Queensland (MUQ), World River Average Clay (WRAC) and East China Post-Archean Shale (ECPAS) (figure 2b and c). The mean Ca and Na were much lower in PIRAC than in UCC and ECPAS. The mean major elements composition of PIRAC and North American Shale composite (NASC) follow each other, except that the Si was slightly lower and Mn higher in PIRAC than in NASC (figure 2c).

The clay fraction (<4 μm size) of sediments was analysed in this study. The near similar major elements contents in APT, DVT and MLT (figure 2a) suggest that the major elements in clay fraction do not show significant variations. Silica-enriched, resistant minerals such as quartz usually occur in coarser grain size fractions of sediments. Low Si in PIRAC compared to the reference sediments may be because of the chemical analyses on clay fraction. Bhuiyan *et al.* (2011) reported low SiO_2/Al_2O_3 ratio in finer grain size fractions of sediments and related to low quartz content in this fraction. Mobile elements such as Na and Ca are easily fractionated during weathering. Marked depletion of Na and Ca in PIRAC relative to reference sediments indicate destruction of feldspars during chemical weathering. The CIA (79.76%) and CIW (87.76%) values of PIRAC indicate moderate chemical weathering on source rocks. Fine-grained sediments comprise abundant clay minerals that usually contain high Fe, Mg and Mn than the bulk sediment. Singh and Rajamani (2001) demonstrated that Fe, Mg, Mn, Ni and Cr tend to be more concentrated in finer than in coarser particles. Relatively high Fe, Mn and Mg in PIRAC compared to the reference sediments (figure 2c) simply suggest more mafic composition of PIRAC. Since these elements are also associated with basic rocks, the influence of basalts should be investigated more thoroughly.

3.2 *Trace elements*

The total trace elements content ($\sum$TE) in the clay fraction of sediments in rivers is shown in figure 3(a). The $\sum$TE was highest for the rivers draining Archean–Precambrian Terrain (APT), followed by those draining the Deccan Trap Volcanic Terrain (DVT) and lowest for the rivers in mixed-lithology terrain (MLT). Among the rivers draining APT, the high $\sum$TE was associated with both medium (Ponnaiyar, Palar) and major (Cauvery) rivers (figure 3a). The average $\sum$TE for the rivers draining APT is highest followed by the rivers draining DVT and then MLT. The $\sum$TE of PIRAC (1724.88 μg/g) is slightly lower than that of PAAS (1807.2 μg/g), close to that of Average Suspended Sediments of the World Rivers (ASSWR – 1725.26 μg/g), but much higher than that of UCC (1650.57 μg/g), NASC (1328.26 μg/g) and MUQ (1257.96 μg/g) (figure 3a). High $\sum$TE contents in the Archean–Precambrian Terrain and Deccan Trap Volcanic Terrain (DVT) were due to very high Cu, Zn and Pb contents.

The variations in the average TE distribution among the three major geological terrains, PIRAC and other reference sediments are shown in figure 3(b–d). Average trace elements distribution showed no significant variations among the three terrains, except that the average Zn, Cu and Pb contents were highest in APT followed by DVT. The trace elements distribution in PIRAC was in between that of APT and DVT with very high Cu, Zn and Pb. PIRAC showed low U, Ta, Hf, Sr, Ba, Nb, Zr and Cs and similar Ni, Sc, Co, Cr, Th, V and Ga contents in comparison to WRAC, ASSWR and NASC. PIRAC showed very high Zn, Cu and Pb, relatively high Ni, Sc, Co, Cr, Th, V, and U and low Rb, Ta, Hf, Sr, Ba, Nb, Zr and Cs in comparison to UCC, MUQ and ECPAS (figure 3d).

Significantly varied $\sum$TE content in rivers among the three geological terrains (figure 3a) implies lithological control on TE content of the sediments. Although the lithology is largely similar, very high $\sum$TE in the Ponnaiyar (medium river) and low $\sum$TE in the Pennar (major) river (figure 3a) suggests that the weathering, mixing and dilution by different sediment types contributed low $\sum$TE in Pennar. In other words, compositions of the clays in the Pennar are modified because of mixing of clays from different sources during long distance transportation. The average CIA (81.7%) and CIW (91.7%) values are highest for the sediments of the rivers draining MLT indicating that the geological formations in this region are subjected to intense chemical weathering. Very low average $\sum$TE in the MLT suggests loss of trace metals to the drainage network during intense weathering and transport. Very high Cu, Zn and Pb in PIRAC relative to other reference sediments indicate that the trace element contents are affected

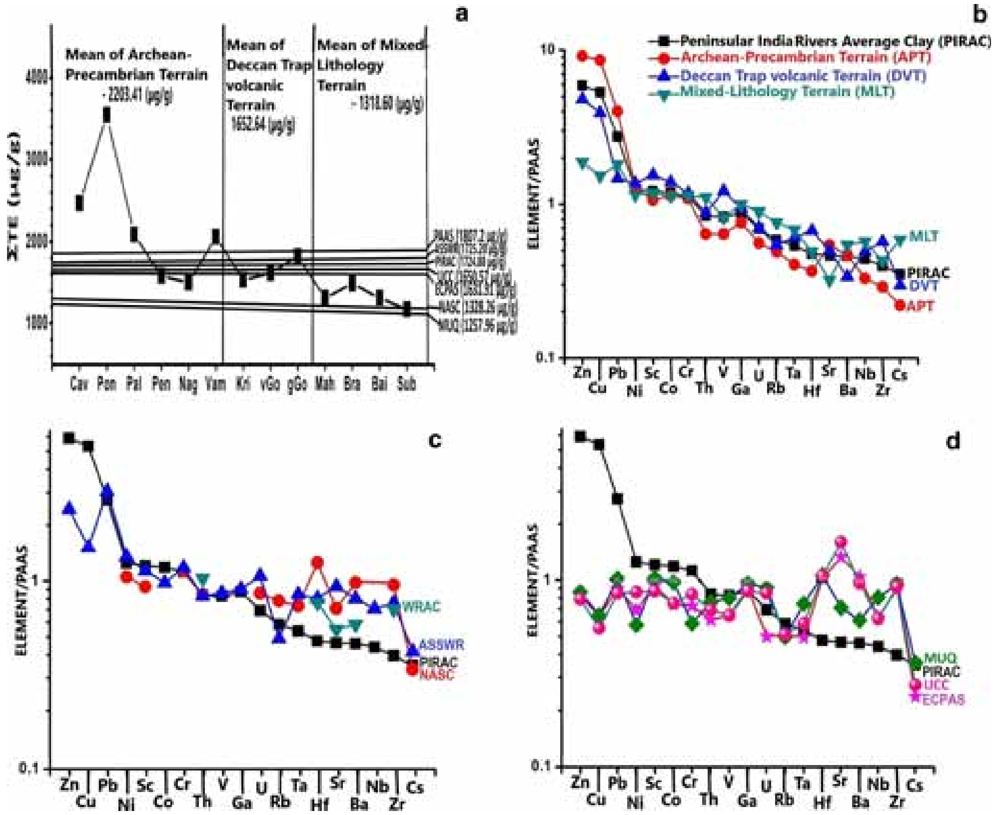

Figure 3. (**a**) Distribution of total trace elements (∑TE) in various rivers (Cau.: Cauvery; Pon.: Ponnair; Pal.: Palar; Pen.: Pennar; Nag.: Nagavali; Vam.: Vamsadhara; Kri.: Krishna; vGo.: Vashista Godavari; gGo.: Gautami Godavari; Mah.: Mahanadi; Bra.: Brahmani; Bai.: Baitarani; Sub.: Subarnarekha). (**b**) Post-Archean average Australian Shale (PAAS)-normalised distribution of trace elements in three major geological formations and PIRAC. (**c** and **d**) PAAS-normalised distribution of trace elements in PIRAC and reference sediments. UCC: Upper Continental Crust, ES: European shale; MUQ: Mud of Queensland, ECPAS: East China Post-Archean Shale, WRAC: World River Average Clay, ASSWR: Average Suspended Sediment of the World Rivers.

by sulphide mineralisation in the source rocks and/or anthropogenic activity (Zhou *et al.* 2004) and are brought by most rivers draining APT and DVT. Thus, these trace elements do not represent crustal composition. Further, the depletion of Rb, Sr, Ba and Cs may be because of loss during leaching under chemical weathering conditions (Zhou *et al.* 2004). Zr and Hf are geochemical twins and associated with heavy minerals. Low concentration of high field strength elements (HFSE) such as Zr, Hf, Nb and Ta (figure 3c–d) are likely controlled by the composition of the catchment and because of low concentrations in clay fraction of sediments. Yang *et al.* (2009) suggested that the heavy minerals are controlled by lithological source and hydrological sorting due to grain size. Similarly, high Ni, Sc, Co, Cr, Th, V and Ga may be because these metals are associated with fine-grained sediments, especially, clay minerals (Hossain *et al.* 2017). Trace metals in this study are affected by both natural and anthropogenic sources of metals, grain size and weathering and thus do not represent the crustal composition.

3.3 *Total rare earth elements (∑REE) content*

The ∑REE of the clay fraction of sediments (figure 4a) indicates that the peaks of high ∑REE are distributed both in major (Gautami Godavari, Mahanadi and Brahmani) and medium (Nagavali and Baitarani) rivers. In contrast to the distribution of ∑TE, the mean ∑REE is lowest for the rivers draining APT, followed by DVT and highest for the rivers draining MLT (figure 4a). The ∑REE of PIRAC is slightly lower than that of PASS but much higher than that of MUQ, ASSWR, NASC, UCC and ECPAS (figure 4a).

Distribution of high and low ∑REE both in medium and major rivers (figure 4a) indicates that the REE abundance is not dependent on the size of the drainage basin or amount of detrital material

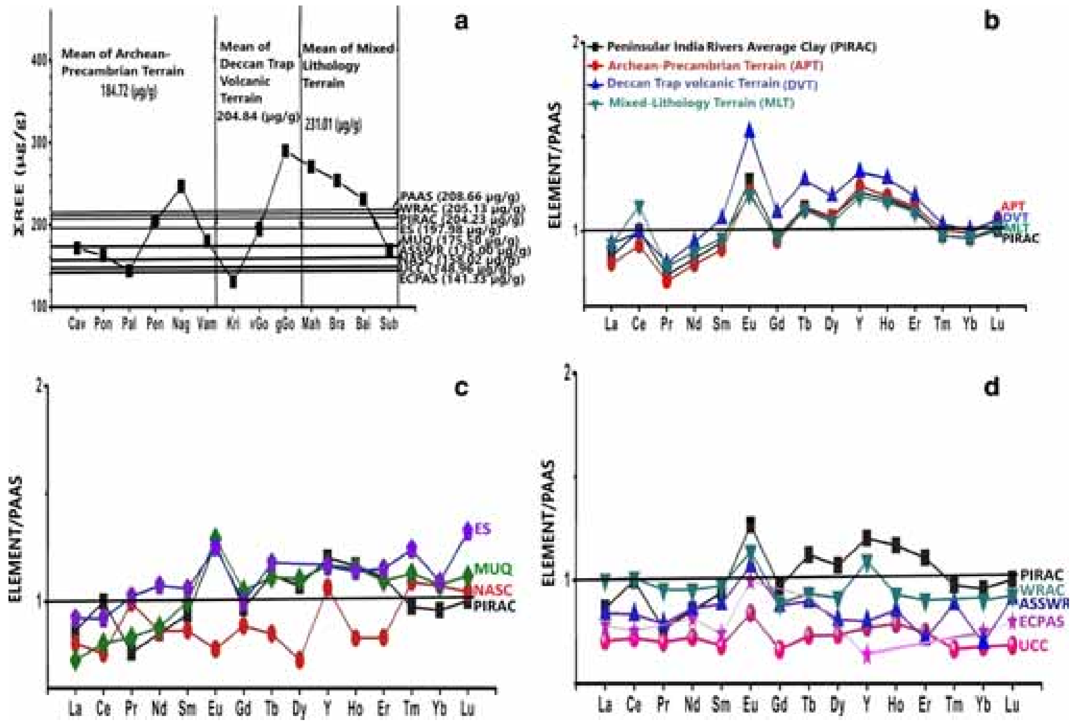

Figure 4. (**a**) Distribution of total rare earth elements (∑REE) in various rivers. (**b**) Post-Archean average Australian Shale (PAAS)-normalised REE patterns in three major geological formations and PIRAC. (**c** and **d**) PAAS-normalised REE patterns in PIRAC and reference sediments. UCC: Upper Continental Crust, ES: European shale, MUQ: Mud of Queensland, ECPAS: East China Post-Archean Shale, WRAC: World River Average Clay, ASSWR: Average Suspended Sediment of the World Rivers.

supplied by rivers. Contrasting distribution of ∑TE and ∑REE in the major geological formations indicate, that unlike TE, ∑REE content may be related to the mineral composition in the terrain. For example, high ∑REE in Nagavali, Baitarani (medium rivers), Mahanadi and Brahmani (major rivers – figure 4a) could be due to the presence of mineral/ore deposits (Konhauser *et al.* 1997). For example, the Nagavali river drains through Precambrian Khondalites consisting of Mn–Fe ores (Moriyama *et al.* 2008). The Mahanadi, Brahmani and Baitarini rivers drain through Fe–Mn and Cr oxide ores and Cu, Zn and Pb sulphide ores in the Singhbhum craton (Konhauser *et al.* 1997; Moriyama *et al.* 2008; Giri *et al.* 2013). The ∑REE of sediments can also be influenced by grain size, heavy minerals and carbonate content of the sediment (Yang *et al.* 2002), and associated with clay minerals and Fe-oxyhydroxides in sediments (Jung *et al.* 2012). Since clay fraction of sediments was analysed in the sediments of all rivers, grain size may not be a factor for variations in ∑REE in our study. However, clay minerals are abundant in <4 μm fraction of sediments and important reservoirs of REEs. Most of the REE reside in clay mineral lattice and a small part as adsorbed onto their surfaces (Taylor and McLennan 1985; Coppin *et al.* 2002).

3.4 *REE patterns*

The PAAS-normalised REE patterns of the clays in three major geological terrains and PIRAC are nearly identical and characterised by LREE depleted and MREE- and HREE-enriched REE patterns with positive Ce and Eu anomalies (figure 4b). The $(La/Yb)_n$, $(Lu/La)_n$, $(La/Sm)_n$ and $(Gd/Yb)_n$ ratios of the PIRAC were 0.9, 1.16, 0.93 and 1.0, respectively (table 1). The REE pattern of PIRAC resembled that of European Shale (ES) and Mud of Queensland (MUQ) (figure 4c), but different from that of WRAC, ASSWR, UCC and ECPAS (figure 4d), which showed LREE-enriched and HREE-depleted REE patterns with very low or no Ce anomaly and positive Eu anomaly (figure 4d).

The PAAS-normalised REE patterns are nearly identical in the three geological terrains. However, it is important to note from table 1, that the $(La/Yb)_n$, $(Lu/La)_n$, $(La/Sm)_n$ and $(Gd/Yb)_n$ ratios of clays show significant variations among the rivers draining APT. The medium rivers with relatively small catchment show more extreme REE patterns varying from LREE- and MREE-enriched and HREE-depleted REE patterns to LREE-depleted and MREE- and HREE-enriched REE patterns. It implies that the medium rivers draining mostly mono-lithology contributed locally to the varied REE patterns. For example, the Ponnaiyar and Palar (medium) rivers drain largely the Archean metamorphic formations and LREE- and MREE-enrichment and HREE-depletion (high $(La/Yb)_n$, $(La/Sm)_n$, $(Gd/Yb)_n$ and low $(Lu/La)_n$ ratios in table 1) in their clays are consistent with their lithology. Similarly, the Nagavali and Vamsadhara (medium) rivers drain the Precambrian Khondalites associated with Mn–Fe ores (Dash *et al.* 1987; Bhattacharya *et al.* 2012) in the Eastern Ghats and LREE-depletion and HREE-enrichment are characteristics of these ores (Moriyama *et al.* 2008; Shynu *et al.* 2013; Prajith *et al.* 2016) and are reflected in their clays (low $(La/Yb)_n$ and high $(Lu/La)_n$ ratios in table 1). Since the abundances of ore deposits are much less compared to the silicate host rocks (khondalites), it is difficult to expect that the REE patterns of clays resembling ore deposits. It is, however, possible because heavy monsoon rains drain both ore deposits and silicate rocks but deposit denser, ore-associated clays closure to the river mouth and transport lighter, silicate-associated clays farther into the sea. The major rivers with large catchment (the Pennar and Cauvery) showed shale-like REE distribution with near equal $(La/Yb)_n$ and $(Lu/La)_n$ ratios (table 1) implying that the sediments are well mixed during long distance transport and these rivers are more effective at REE averaging. Further, the average REE composition of clays of all 6 rivers draining APT exhibits LREE-depleted and MREE- and HREE-enriched REE patterns with positive Ce and Eu anomalies (figure 4b). It implies that the weathering products are dominated by the felsic component of the metamorphic rocks and ore deposits and reflected in the average clays from the Archean-Precambrian Terrain.

The Krishna, Vasishta Godavari and Gautami Godavari drain dominantly the Deccan Trap volcanic Terrain (DVT) in the upper reaches and gneissic rocks and deltaic sediments in the lower reaches (figure 1; Krishnan 1968). The REE patterns exhibit LREE-depleted and HREE-enriched patterns with positive Ce and Eu anomalies (figure 4a). HREE-enriched REE patterns with positive Eu anomaly have been reported for the clays weathered from volcanic rocks (Goldstein and Jacobsen 1988; Ross *et al.* 1995; Bayon *et al.* 2015). Positive Ce anomaly is not characteristic of volcanic rocks. Since positive Ce anomaly is also present in the average DVT, the REE pattern may represent mixed pattern from both volcanic and metamorphic rocks. The average DVT exhibiting HREE-enriched patterns suggests the sediment load from volcanic rocks abundantly deposited in the lower reaches of the river. This is because volcanic rocks are more widespread spatially in the drainage basin and are more easily weathered than the metamorphic rocks.

The Mahanadi, Brahmani, Baitarini and Subarnarekha rivers drain through mixed-lithology terrain (MLT) such as metamorphic and igneous rocks, consisting of ore deposits of both (Fe–Mn) oxides and (Cu–Pb) sulphides in the upper reaches, laterites and different soils (lateritic, yellow and red) and deltaic sediments in the lower reaches (Dash *et al.* 1987). The detrital clay fraction at the river end is therefore an admixture, characterised by MREE-enriched and near equal proportions of LREE and HREE (table 1) indicating that the REE of the clays are averaged out during transportation and deposition. The average REE composition of the MLT is LREE-depleted and MREE- and HREE-enriched REE patterns (figure 4b).

The PAAS-normalised REE pattern of PIRAC represents the average REE composition of clays in 13 rivers and characterised by LREE-depletion and MREE- and HREE-enrichment with positive Ce and Eu anomalies. The REE pattern of PIRAC resembles that of European shale (ES) and Mud of Queensland (MUQ), except in the absence of significant Ce anomaly in ES and MUQ (figure 4c). The REE pattern of PIRAC is different from that of WRAC, UCC, NASC and ECPAS which exhibit LREE-enriched and HREE-depleted REE pattern (figure 4d). Although the Archaean and Precambrian metamorphic crust is voluminously abundant in the drainage basins of several rivers, the MREE- and HREE-enriched pattern in PIRAC is conspicuous. It may not due to the analysis of clay fraction of sediments in this study, as this size fraction is slightly enriched with MREE- and HREE because of weathering (Nesbitt *et al.* 1990; Bayon *et al.* 2015) or, river clays are generally enriched in MREE, most likely caused by the weathering of phosphate minerals (Hannigan and Sholkovitz 2001). Moreover, Bayon *et al.* (2015) also investigated REE patterns of the clay factions of sediments in world rivers exhibiting LREE- and MREE-enriched and HREE-depleted REE patterns. Other shales such as, the ES and MUQ also exhibit HREE-enriched patterns. The MREE- and HREE-enrichment in PIRAC may be related to the weathering on source rocks and rapid transportation of clays from the soils during monsoon season. We therefore suggest that the weathering products from volcanic rocks and felsic component of metamorphic rocks dominantly transported and deposited at the river mouth. In other words, the crustal composition of the peninsular India differs from that of other reference sediments and it should be thoroughly investigated with more analyses to better understand the composition of the upper crust of the Indian subcontinent.

4. Conclusions

We present a new dataset on the average composition of the clay fraction of sediments in 13 rivers draining the entire peninsular India, referred to here as Peninsular India Rivers Average Clay (PIRAC) that represents the crustal composition of peninsular India. PIRAC showed

(i) low Si and high Fe, Mn and Mg compared to other reference sediments.
(ii) slightly lower total trace element ($\sum$TE) and $\sum$REE contents than in PAAS but much higher than in UCC, ES, ECPAS and WRAC.
(iii) characteristically high Cu, Zn and Pb.
(iv) LREE-depleted, MREE- and HREE-enriched REE patterns with positive Ce and Eu anomaly upon PAAS-normalisation.

The REE pattern of PIRAC resembles that of European Shale and Mud of Queensland, but different from that of UCC, PAAS, ECPAS, WRAC and ASSWR, which exhibit LREE-enriched and HREE-depleted REE patterns. Therefore, it is necessary to determine the crustal composition of PIRAC with more number of analyses to better understand the chemical evolution of the crust.

Acknowledgements

We wish to thank the Vice-Chancellor, VFSTR, Vignan's University, Vadlamudi and Director, CSIR–National Geophysical Research Institute (CSIR–NGRI) for facilities and encouragements. V P Rao wishes to thank CSIR, New Delhi for Emeritus Scientist Fellowship. Mr Sai Babu thanks VU for the Junior Research Fellowship. We thank the JESS reviewers for critically going through the manuscript and giving suggestions.

References

Absar N, Raza M, Roy M, Naqvi S M and Roy A K 2009 Composition and weathering conditions of Paleoproterozoic upper crust of Bundelkhand craton, central India: Records from geochemistry of clastic sediments of 1.9 Ga Gwalior Group; *Precamb. Res.* **168(3)** 313–329.

Absar N and Sreenivas B 2015 Petrology and geochemistry of greywackes of the ∼1.6 Ga Middle Aravalli Supergroup, northwest India: Evidence for active margin Processes; *Int. Geol. Rev.* **57** 134–158.

GSI 1998 *Geological map of India*; 7th edn, Geological Survey of India, Bangalore.

Balakrishnan S and Rajamani V 1987 Geochemistry and petrogenesis of granite gneisses around the Kolar Schist Belt, south India: Petrogenetic constraints for the evolution of the crust in the Kolar area; *J. Geol.* **95** 219–240.

Bayon G, Toucanne S, Skonieczny C, André L, Bermell S, Cheron S, Dennielou B, Etoubleau J, Freslon N, Gauchery T, Germain Y, Jorry S J, Ménot G, Monin L, Ponzevera E, Rouget M L, Tachikawa K and Barrat J A 2015 Rare earth elements and neodymium isotopes in world river sediments revisited; *Geochim. Cosmochim. Acta* **170** 17–38.

Bhatia M R 1985 Rare earth element geochemistry of Australian Paleozoic graywackes and mudrocks: Provenance and tectonic controls; *Sedim. Geol.* **45** 97–113.

Bhattacharya S, Chaudhary A K and Basei M 2012 Original nature and source of khondalites in the Eastern Ghats Province, India; In: *Palaeoproterozoic of India* (eds) Mazumder R and Saha D, *Geol. Soc. London, Spec. Publ.* **365** 147–159.

Bhuiyan M A H, Rahman M J L, Dampare S B and Suzuki S 2011 Provenance, tectonics and source weathering of modern fluvial sediments of the Brahmaputra–Jamuna River, Bangladesh: Inference from geochemistry; *J. Geochem. Explor.* **111** 113–137.

Cullers R L, Chaudhury S, Kilbane N and Koch R 1979 Rare earths in size fractions and sedimentary rocks of Pennsylvanian–Permian age from the mid-continent of the USA; *Geochim. Cosmochim. Acta* **43** 1285–1301.

Condie K C 1993 Chemical composition and evolution of the upper continental crust: Contrasting results from surface samples and shales; *Chem. Geol.* **104** 1–37.

Coppin F, Berger G, Bauer A, Caslet S and Loubet M 2002 Sorption of lanthanides on smectite and kaolinite; *Chem. Geol.* **182** 57–68.

Dash B, Sahu K N and Bowes D R 1987 Geochemistry and original nature of Precambrian khondalites in the Eastern Ghats, Orissa, India; *Trans. Roy. Soc. Edinburgh* **78** 115–127.

Gao S, Luo T C, Zhang B R, Zhang H F, Han Y W, Hu Y K and Zhao Z D 1998 Chemical composition of the continental crust as revealed by studies in east China; *Geochim. Cosmochim. Acta* **62** 1959–1975.

Giri S, Singh A K and Tewary B K 2013 Source and distribution of metals in bed sediments of Subarnarekha River, India; *Environ. Earth Sci.* **70** 3381–3392.

Goldstein S J and Jacobsen S B 1988 Rare earth elements in river waters; *Earth Planet. Sci. Lett.* **89** 35–47.

Gromet L P, Dymek R F, Haskin L A and Korotev R L 1984 The North American shale composite: Its compilation, major and trace element characteristics; *Geochim. Cosmochim. Acta* **48** 2469–2482.

Hannigan R E and Sholkovitz E R 2001 The development of middle rare earth element enrichments in freshwaters: Weathering of phosphate minerals; *Chem. Geol.* **175** 495–508.

Haskin M A and Haskin L A 1966 Rare earths in European shales: A redetermination; *Science* **154** 507–509.

Hossain Z H M, Kawahata H, Roser B P, Sampei Y, Manaka T and Otani S 2017 Geochemical characteristics of modern river sediments in Myanmar and Thailand: Implications for provenance and weathering; *Chemie der Erde,* http://dx.doi.org/10.1016/j.chemer.2017.07.005.

Jung H S, Lim D, Choi J Y, Yoo H S, Rho K C and Lee H B 2012 REE compositions of core sediments from the shelf of the South Sea, Korea: Their controls and origins; *Cont. Shelf Res.* **48** 75–86.

Kamber B S, Greig A and Collerson R D 2005 A new estimate for the composition of weathered young upper continental crust from alluvial sediments, Queensland, Australia; *Geochim. Cosmochim. Acta* **69** 1041–1058.

Konhauser K O, Powell M A, Fyfe W S, Longstaffe F J and Tripathy S 1997 Trace element chemistry of major rivers in Orissa State, India; *Environ. Geol.* **29** 132–141.

Krishnan K S 1968 *Geology of India and Burma*; Higginbottoms, Madras, 536p.

Marchandise S, Robin E, Ayrault S and Roy-Barman M 2014 U–Th–REE–Hf bearing phases in Mediterranean Sea sediments: Implications for isotope systematics in the ocean; *Geochim. Cosmochim. Acta* **131** 47–61.

McLennan S M 2001 Relationship between the trace element composition of sedimentary rocks and upper continental crust; *Geochem. Geophys. Geosyst.* **2** 2000GC000109.

Moriyama T, Panigrahi M K, Pandit D and Watanabe Y 2008 Rare earth element enrichment in Late Archean manganese deposits from the Iron Ore Group, East India; *Resour. Geol.* **58** 402–413.

Nance W B and Taylor S R 1976 Rare earth element patterns and crustal evolution – I. Australian post-Archean sedimentary rocks; *Geochim. Cosmochim. Acta* **61** 1539–1551.

Naqvi S M 2005 *Geology and Evolution of the Indian Plate (from Hadean to Holocene 4 Ga to 4 Ka)*; Capital Publishing Company, New Delhi, 450p.

Nesbitt H W, MacRae N D and Kronberg B I 1990 Amazon deep-sea fan muds: Light REE enriched products of extreme chemical weathering; *Earth Planet. Sci. Lett.* **100** 118–123.

Pourmand A, Dauphas N and Ireland T J 2012 A novel extraction chromatography and MC-ICP-MS technique for rapid analysis of REE, Sc and Y: Revising CI-chondrite and Post-Archean average Australian Shale (PAAS) abundances; *Chem. Geol.* **291** 38–54.

Prajith A, Rao V P and Chakraborty P 2016 Distribution, provenance and early diagenesis of major and trace metals in sediment cores from the Mandovi estuary, western India; *Estuar. Coast Shelf Sci.* **170** 173–185.

Rashid S A, Ahmad S, Singh S K and Absar N 2018 Elemental and Sr–Nd isotopic geochemistry of Mesoproterozoic sedimentary successions from NE Lesser Himalaya, northern India: Implications for Proterozoic climate and tectonics, *J. Asian Earth Sci.* **163** 235–248.

Rao K L 1975 *India's Water Wealth*; Orient Longman Ltd., Hyderabad.

Ray S B, Mohanti M and Somayajulu B L K 1984 Suspended matter, major cations and dissolved silicon in the estuarine waters of the Mahanadi river, India; *J. Hydrol.* **69** 183–196.

Ross G R, Guevara S R and Arribére M A 1995 Rare earth geochemistry in sediments of the Upper Manso River Basin, Rio Negro, Argentina; *Earth Planet. Sci. Lett.* **133** 47–57.

Rudnick R L and Gao S 2003 The composition of the continental crust; In: *Treatise on Geochemistry* (eds) Rudnick R L, Holland H D and Turekian K T, Vol. 3, Elsevier Pergamon, Oxford, pp. 1–64.

Satyanarayanan M, Balaram V, Sawant S S, Subramanyam K S V, Vamsi Krishna G, Dasaram B and Manikyamba C 2018 Rapid determination of REEs, PGEs, and other trace elements in geological and environmental materials by high resolution inductively coupled plasma mass spectrometry; *Atomic Spectrosc.* **39** 1–15.

Sharma A and Rajamani V 2000 Weathering of gneissic rocks in the upper reaches of Cauvery River, South India: Implications to neo-tectonics of the region; *Chem. Geol.* **166** 203–223.

Shynu R, Rao V P, Parthiban G, Balakrishnan S, Narvekar T and Kessarkar P M 2013 REE in suspended particulate matter and sediment of the Zuari estuary and adjacent shelf, western India: Influence of mining and estuarine turbidity; *Mar. Geol.* **346** 326–342.

Singh P and Rajamani V 2001 REE geochemistry of recent clastic sediments from the Kaveri floodplains, southern India: Implication to source area weathering and sedimentary processes; *Geochim. Cosmochim. Acta* **65** 3093–3108.

Srinivasan R, Naqvi S M, Uday Raj B, Subbarao D V, Balaram V and Rao T G 1989 Geochemistry of the Archaean greywackes from the north western part of Chitradurga schist belt, Dharwar Craton, south India – evidence for granetoid upper crust in the Archaean; *J. Geol. Soc. India* **34** 505–516.

Taylor S R and McLennan S M 1985 *The Continental Crust: Its Composition and Evolution. An Examination of the Geochemical Record Preserved in Sedimentary Rocks*; Blackwell Scientific Publications, Oxford, 312p.

Viers J, Dupré B and Gaillardet J 2009 Chemical composition of suspended sediments in World Rivers: New insights from a new database; *Sci. Total Environ.* **407** 853–868.

Yang S Y, Jung H S, Choi M S and Li C X 2002 The rare earth element compositions of the Changjiang (Yangtze) and Huanghe (Yellow) river sediments; *Earth Planet. Sci. Lett.* **201** 407–419.

Yang S, Wang Z, Guo Y, Li C and Cai J 2009 Heavy mineral compositions of the Changjiang (Yangtze River) sediments and their provenance-tracing implication; *J. Asian Earth Sci.* **35** 56–65.

Zhao and Zheng 2015 The intensity of chemical weathering: Geochemical constraints from marine detrital sediments of Triassic age in South China; *Chem. Geol.* **391** 111–122.

Zhou H-Y, Peng Z-T and Pan J-M 2004 Distribution, source and enrichment of some chemical elements in sediments of the Pearl River Estuary, China; *Cont. Shelf Res.* **24** 1857–1875.

Corresponding editor: Santanu Banerjee